Journal of Experimental and Theoretical Physics, Vol. 100, No. 4, 2005, pp. 637–644.
From Zhurnal Éksperimental'noĭ i Teoreticheskoĭ Fiziki, Vol. 127, No. 4, 2005, pp. 723–731.

NUCLEI, PARTICLES, FIELDS, GRAVITATION, AND ASTROPHYSICS

Redshifts in Space Caused by Stimulated Raman Scattering in Cold Intergalactic Rydberg Matter with Experimental Verification¶

L. Holmlid

Atmospheric Science, Department of Chemistry, Göteborg University, SE-412 96 Göteborg, Sweden
e-mail: holmlid@chem.gu.se

Received September 23, 2004

Abstract—The quantized redshifts observed from galaxies in the local supercluster have recently been shown to be well described by stimulated Stokes Raman processes in intergalactic Rydberg matter (RM). The size of the quanta corresponds to transitions in the planar clusters forming the RM, of the order of 6×10^{-6} cm^{-1}. A stimulated Stokes Raman process gives redshifts that are independent of the wavelength of the radiation, and it allows the radiation to proceed without deflection, in agreement with observation. Such redshifts must also be additive during the passage through space. Rydberg matter is common in space and explains the observed Faraday rotation in intergalactic space and the spectroscopic signatures called unidentified infrared bands (UIBs) and diffuse interstellar bands (DIBs). Rydberg matter was also recently proposed to be baryonic dark matter. Experiments now show directly that IR light is redshifted by a Stokes stimulated Raman process in cold RM. Shifts of 0.02 cm^{-1} are regularly observed. It is shown by detailed calculations based on the experimental results that the redshifts due to Stokes scattering are of at least the same magnitude as observations. © *2005 Pleiades Publishing, Inc.*

1. INTRODUCTION

The redshifts observed from distant extragalactic sources in space are quite intriguing, and their origin has been debated by many authors. The important reports that the redshifts are quantized [1, 2] are at variance with the accepted interpretation of the redshifts. The quantization of galactic redshifts was recently shown to agree with the expected stimulated Raman process in intergalactic Rydberg matter (RM) [3]. That intergalactic matter exists at nonnegligible densities is shown, for example, by the observation of a Faraday rotation effect at radiofrequencies in intergalactic space [4]. This effect is well described by very low densities of RM, with its high electron density and inherent magnetic field [5]. It is also proposed that RM is the (baryonic) dark matter in space [6]. The properties of RM are such that it is an excellent candidate for the missing dark matter. For example, a hydrogen atom in RM takes up a volume 5×10^{12} times larger than a ground-state hydrogen atom.

Rydberg matter is a special form of matter, which is built up of weakly interacting, highly excited atoms or molecules in circular, metastable Rydberg states. It has metallic properties due to the delocalized electrons and a very low density under the conditions in space. We have shown that low-density RM can be conveniently studied by laser fragmentation and time-of-flight methods [7–9]. Rydberg matter can be built up from alkali atoms and also from small gas molecules like H_2 and N_2 [8, 10, 11]. It can also be formed from H atoms [12, 13]. The existence and structure of RM was predicted by Manykin, Ozhovan and Poluéktov [14, 15] more than 20 years ago, and by 1991, the first experimental studies of a macroscopic Cs Rydberg matter phase were performed [16, 17]. These early studies of RM have recently been independently confirmed [18]. Improved quantum mechanical calculations of the properties of RM built up by Cs were also published [19, 20]. Later, studies by time-of-flight methods [7, 10, 21] identified the special planar cluster shapes predicted by theory [22]. The distance between the ions in the RM can be measured by the repulsion energy released in Coulomb explosions in the matter [8, 9, 11, 12]. This bond distance is a few nanometers at the relatively low excitation levels studied by this technique.

Due to the extremely large polarizability of RM, Raman spectroscopic studies will be very useful to find information on the properties of RM. A blueshift of single-mode IR laser light passing through RM was observed and interpreted as an anti-Stokes stimulated electronic Raman effect (ASERS) [23]. Experiments have also directly observed anti-Stokes Raman scattering from RM surface layers. Transitions in K Rydberg atoms [24] and bands from H_2 and other small molecules, and bands from transitions in the RM [25] were observed. The stimulated Raman effect was also used in a micro-Raman spectroscopy study of the interaction of

¶ This article was submitted by author in English.

water molecules with one of the solid materials used to emit RM in laboratory [26]. A recent study interpreted the interaction observed between laser modes observed in transmission and reflection of IR lasers in RM as being due to the stimulated Raman effect [27]. Another method recently employed for the study of RM is stimulated emission, which works well due to extremely long lifetimes of the electronically excited states in RM. In fact, the first thermally excited laser was recently demonstrated in the IR range [28, 29]. This CW laser is tunable over the range 800–14000 nm. The numerous bands observed in the stimulated transitions agree with the transitions expected in RM.

The lifetime of RM is very long in space, which allows its rate of formation to be very low. Extrapolation from the theoretical results in [20] gives a radiative lifetime of undisturbed RM of the order of the lifetime of the universe. That RM is a common type of matter in space is shown by the interpretation [30] of the unidentified infrared bands (UIR, UIB) as being due to transitions in RM, in fact, the same transitions experimentally studied by stimulated emission [29] and by a few stimulated Raman experiments [24, 25]. Further evidence comes from the Faraday rotation observations in intergalactic space and their interpretation as being due to RM [5]. More evidence also exists. A large number (at least 60) of the so-called diffuse interstellar bands (DIBs) have been calculated accurately using a theory based on the RM concept [31].

Because the conduction band in RM is not filled, almost continuous electronic excitations are possible. In a stimulated electronic Raman process, a photon gains or loses some energy from the interaction with matter, and RM may then change the frequency of radiation passing through it by very small amounts, in the form of a red or blue shift (Stokes or anti-Stokes shifts) of the radiation. A blueshift was observed in the experiments in [23], where the RM used was electronically excited by its formation process and by the high temperature of the surrounding equipment. This shift is expected to change to a redshift as in Stokes scattering in cold RM in space. Further experiments using the same technique have recently been published [32]. In that study, redshifts were observed in reflection from a layer of cold RM deposited on a window. We now demonstrate directly that a redshift is observed in cold RM even in transmission. Redshifts of the radiation from distant galaxies are found from the interaction between radiation and RM, as explained in [3].

2. THEORY

In what follows, the term light is used for simplicity in many places where the term electromagnetic radiation could be used instead.

2.1. Estimated Gain

An important process for the interaction between light and RM is the stimulated electronic Raman scattering of the Stokes or anti-Stokes type (SERS, ASERS) [33]. Anti-Stokes Raman scattering and similar processes in RM have been observed in different types of experiments [24, 25, 34], even at low light intensities [23, 26, 27]. For cold ground-state RM, Stokes scattering should be observed instead. There is no phase matching condition for this type of process [33], and the Raman-scattered light proceeds in the same direction as the incident light.

It is necessary to estimate the magnitude of the stimulated Raman effect in the case of an RM material. For this, we use the ordinary classical steady-state gain factor derived for molecular vibrational transitions. The formulas are given for the Stokes scattering, which is the case of interest for astrophysical processes. The equations are identical in form for the anti-Stokes (*as*) and Stokes (*s*) cases. The incident light frequency is ω_L and the generated Stokes wave has a frequency ω_s. The difference

$$\omega_L - \omega_s = \omega_E$$

is the resulting electronic excitation in the RM material. For the Stokes wave, the steady-state gain factor G_{ss} at its maximum is given by [35]

$$G_{ss} = \frac{N_d k_s}{8m\epsilon\gamma(\omega_L - \omega_s)}\left(\frac{\partial\alpha}{\partial q}\right)_0^2 |E_L|^2. \quad (1)$$

In this expression N_d is the density of the dipoles created by the incident light wave, here chosen to correspond to the number of electrons in the RM; k_s is the wavenumber for the Stokes wave; m is the mass of the driven oscillator, in this case, one electron mass; $\epsilon = \epsilon_r\epsilon_0$ is the permittivity of the medium, which is unknown but probably has ϵ_r on the order of unity; γ is the coupling constant for the electronic excitation in the intermediate state to other degrees of freedom; $\partial\alpha/\partial q$ is the variation of the polarizability with the coordinate describing the excited motion, here the electronic motion; and E_L is the electric field strength of the incident light.

The gain factor G_{ss} can be large even at low light intensities due to the very large polarizability of the RM and an arbitrarily small value of the difference $\omega_L - \omega_s$. The reason for this small value is the almost continuous nature of the energy levels in RM. Another factor of great importance is the coupling (dephasing) constant γ, which is much smaller than in the case of ordinary matter because the coupling of the electronic motion in RM to other modes of motion is weak. From the experiments with IR lasers, it was concluded that γ is on the order of 10^3 s^{-1} or smaller [23]. This would give a lower

limit on the magnitude of the electronic excitations in terms of wavenumbers from

$$c\Delta\tilde{\nu} = \omega_E \gg \gamma \text{ as } \Delta\tilde{\nu} \gg 3\times10^{-8}\ \text{cm}^{-1}.$$

The quantized redshifts interpreted in [3] give

$$\Delta\tilde{\nu} \approx 6\times10^{-6}\ \text{cm}^{-1}$$

in agreement with the experimentally found lower limit for γ. We use this value as a reasonable quantum magnitude of the electronic excitation in RM above each metastable state with a certain excitation level n. Lifetime measurements of RM both at 77 K [36] and at 800 K [16, 37] and calculations at low excitation levels [20] seem to indicate a much smaller value of γ, maybe on the order of 10^{-3} s^{-1} [23, 34]. However, these lifetimes probably correspond to deexcitation from an excitation level n down to the fully dissociated ground state consisting of separate atoms or molecules.

To estimate reasonable values of the quantities in Eq. (1), we use a phase of RM with the excitation state $n = 80$, which is the average value deduced from the study in [30]. Each Rydberg atom is then considered a polarizable particle. With interatomic distances of 0.5 μm at $n = 80$, the density is found to be approximately 10^{18} m^{-3}. The wavenumber k_s is on the order of 2×10^4 cm^{-1} or 2×10^6 m^{-1} in the visible range, and the difference of the frequencies $\omega_L - \omega_s$ is assumed to be 10^{-6} cm^{-1} or 10^{-4} m^{-1}. In fact, with RM, this value is probably even smaller. The mass m is the electron mass and ϵ is the dielectric constant ϵ_r times ϵ_0. The polarizability variation $\partial\alpha/\partial q$ is estimated as the volume added for a change in the radial distance for the Rydberg electron (times ϵ_0 to give the right dimension) and becomes 4.4×10^{-24} As m V^{-1}. Finally, the field strength due to light is estimated for the power density 1 mW cm^{-2}, giving $E = 90$ V m^{-1}. This gives

$$G_{ss} = \frac{3\times10^{17}}{\epsilon_r\gamma}\ \text{m}^{-1} \qquad (2)$$

with γ in s^{-1} and ϵ_r on the order of unity. Even for rather large values of γ, the G_{ss} factor is large, which means that the stimulated Raman effect is strong and an efficient conversion to the Stokes wave takes place in a short distance. It may be assumed that γ is of the order of 10^3 s^{-1}. This means that the G_{ss} factor is very large and gives rise to a strong stimulated effect by the equation for the Stokes field strength [33, 35]

$$E_s^f = E_s(0)\exp(G_{ss}x), \qquad (3)$$

where the index f indicates a forward wave, $E_s(0)$ is the Stokes wave at position zero (noise photons), and x is the distance along the laser beam. Thus, it is obvious that stimulated Raman effects should be observable even for low light intensities, especially if x is very large as in intergalactic space.

2.2. Continuous Excitations

The form of Eq. (1) is best suited for molecular vibrational Raman problems. Other forms of this equation exist (as, e.g., in [38]) which in general are better suited for electronic excitations. However, the theory of RM shows that the delocalized electrons, as in ordinary Rydberg states, are close to the classical limit. For example, in [22], the bond energies and electronic levels of RM are calculated from electrostatic formulas, only with the addition of the electron correlation as a quantum mechanical effect. The transitions of interest here, between translational states of the RM electrons in the RM clusters, have very small quanta and are almost classical in nature. This means that a description of the interaction between the light wave and the molecular system in terms of motion of point particles, like in the vibrational Raman transitions, is quite well adapted to RM electronic excitations.

In the case of stimulated Raman scattering, well-defined Raman transitions are normally studied, and not a continuous range of wavenumbers ω_E. Because one well-defined Stokes (or anti-Stokes) frequency usually dominates and gives the Raman wave, it is not directly clear what happens if a range of transitions is possible. In the present case, consecutive Stokes components are formed along the laser beam, as shown, for example, in [33, 39]. If a range of frequencies is possible, this could be thought to lead to a broadening of the Stokes wavevector and a less well-defined stimulated Raman appearance. From Eq. (3), however, one can see that the switch from one Stokes component to the next occurs when the exponent $G_{ss}x$ is sufficiently large. Because

$$G_{ss}x \propto \frac{x}{\omega_E},$$

a smaller value of ω_E gives the same value of the exponent in a proportionally shorter distance x. This means that if a smaller ω_E takes over, it switches over to the next Stokes component faster, keeping the resulting shift after a larger distance constant, independently of which ω_E actually dominates. This shows that the detailed process of the Stokes component switching with a continuous range of transitions is of no great concern, because the result is the same.

2.3. Intensity Dependence

The small value of γ means that the form of G_{ss} given by Eq. (1) is not strictly valid. Assuming that this effect does not change the theoretical formulas completely, one can still use the treatment by Shen and

Bloembergen [39] and Shen [38] to find a more complete description of the Raman signal. For a small wave vector momentum mismatch along the light direction (the *x*-direction)

$$\Delta k = 2k_{L(x)} - k_{s(x)} - k_{as(x)},$$

the gain is observed to decrease linearly towards zero as $\Delta k \longrightarrow 0$. The plots for this effect are given as reduced plots in [39] and also in [23], where the scales of both axes are in reduced quantities, relative to G_{ss}. Because G_{ss} is proportional to $|E_L|^2$, an increase in the light intensity increases G_{ss} and thus moves a point on the curve downwards, for constant Δk. This means that the relative gain decreases by the same factor, keeping the real gain G constant. Thus, the gain G varies linearly with the mismatch Δk. The gain G is then independent of the light intensity for constant Δk in the region of small momentum mismatch, which probably is the range of interest for space. Because the value of G_{ss} is extremely large, as described above, the resulting gain can still be substantial. The analysis in [38, 39] shows further that the anti-Stokes wave formed together with the Stokes wave has a lower intensity at relatively small values of Δk.

3. RESULTS

3.1. Cold Rydberg Matter in the Laboratory

Rydberg matter can be produced by several techniques in the laboratory in different surroundings and from different starting materials [40]. Usually, the formation process involves relatively high temperatures, from 300 K up to 1500 K depending on the technique used. This means that the RM produced is in an electronically excited state with electron translation in the RM cluster above its ground state, which is characterized by a certain principal quantum number *n*. The reason for the excitation is that the RM is formed in the experiments by condensation of excited clusters, molecules, and atoms in Rydberg states. The excess energy in the RM clusters comes from the condensation energy and from collisions with an excitation energy transfer from the Rydberg species. However, a cooling process can be applied to reach lower electronic temperatures. At RM densities of interest in space, the condensed phase consists mainly of hexagonal planar clusters with the magic number (number of members in a stable cluster) N = 7, 19, 37, 61, and 91 as observed experimentally [7, 11].

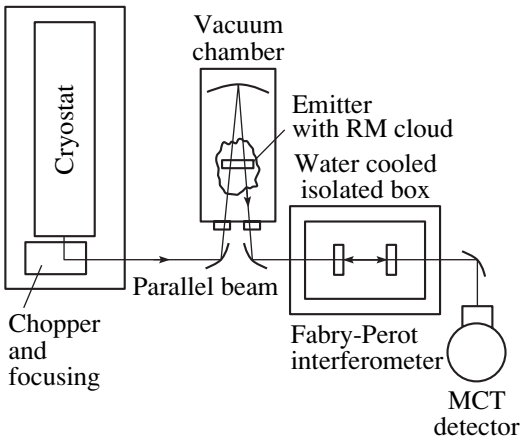

Fig. 1. Block diagram of the experimental setup for a transmission measurement. The RM cloud around the hot emitter is indicated.

In the present stimulated Raman experiment, an almost single-mode CW laser with mW power is used in the IR range, with ω_L close to 1100 cm^{-1}. The slope of the laser modes is approximately 7×10^{-3} cm^{-1} mA^{-1}. The setup is similar to the one used in [23, 32] with an air-spaced Fabry–Perot interferometer (FPI) with ZnSe mirrors between the RM chamber and the detector. A mirror is used inside the RM chamber to reflect the laser beam passing below the RM emitter. See Fig. 1. After formation, the RM cloud is allowed to cool itself with the RM emitter turned off. The lifetime of RM in the laboratory under these conditions is of the order of a few hours. As observed directly in laser fragmentation experiments, the cold RM gives translational temperatures of a few K for large clusters [9, 11]. This cooling is probably driven by stimulated emission in the IR range [29]. The result of this cooling process is that a redshift of the light passing through the RM cloud can be detected with the interferometer.

A typical result with blueshifting (leftshift) at a high emitter temperature due to the formation of a cloud of warm RM is shown in Fig. 2. At the end of the experiment, a redshift (rightshift) is observed after cooling of the RM. A complete run with less blueshifting due to colder RM (exhausted RM emitter) is shown in Fig. 3. Time and FPI temperature are given in the figure. A temperature-stable (often water-cooled) FPI with an Invar base, usually in a well insulated box was used, with a free spectral range of 0.19 cm^{-1}. The temperature coefficient of the FPI is determined to be less than 1.5×10^{-2} cm^{-1} K^{-1}. This gives an elongation of the cavity with increasing temperature and a drift of the peaks (fringes) to the left in the figure. Thus, the true redshift in the figures (rightshift) is slightly larger than directly observed because the temperature of the FPI increased during the experiment. The redshift observed is of the order of 0.02 cm^{-1} for a passage with length of the order of 25 cm through RM in a surrounding air pressure of 10^{-4} mbar. It is estimated that the density of RM is close to the gas density in the chamber. This gives a value of 10^{18} m^{-3} if RM fills the volume almost completely, with the excitation level n = 80. Due to the planar cluster structure of RM, a filling factor of 10% is more likely, giving the density 10^{17} m^{-3} in the experiments.

A redshifting of the interferometer fringes can also be observed with cold RM deposited on the inner surface of the ZnSe window used in the RM chamber. The window is antireflection-coated on the outer surface, and the reflection on the inner surface is observed. This effect was demonstrated in [32]. In this configuration, only the evanescent wave interacts with the cold RM on the inner surface. A similar configuration was shown to work well in stimulated emission experiments using RM [41], where the coupling to the external laser cavity took place via the evanescent wave. The results from a reflection experiment are shown in Fig. 4. The noise in the signal is relatively high because just a fraction of the laser beam intensity is reflected. The time for the scans and the temperature of the mirror holder in the FPI are shown. A redshift (rightshift) is seen, caused by the deposition of RM on the window during heating of the RM emitter. After return to room temperature, the redshift gradually disappears and after two hours, the shift is zero. We note that the FPI temperature is still higher than initially and that the drift of the fringes due to temperature changes of the FPI is thus small. A more complete discussion of the influence of temperature changes of the FPI is given in [32].

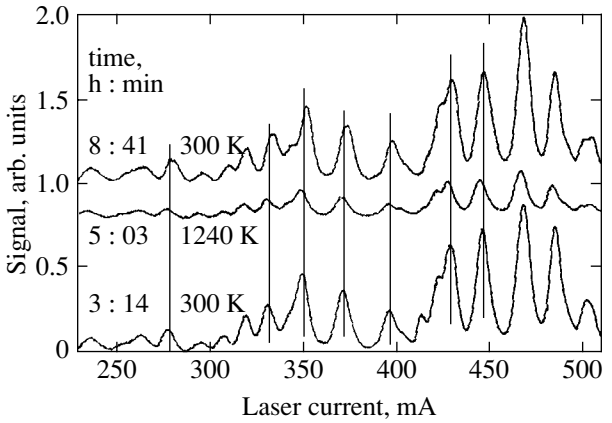

Fig. 2. Initial blueshift due to warm RM and final redshift due to cold RM of light from a diode laser at 1100 cm^{-1} passing through the RM cloud. The lower trace is taken with the RM emitter at room temperature, while the top one is after heating to 1240 K and subsequent cooling, at an air pressure of 10^{-4} mbar in the RM chamber. Note the blueshift at 1240 K and the redshift (rightshift) in the top curve. The same data as in [32].

3.2. Cold Rydberg Matter in Space

In space, Rydberg matter can exist both at low temperatures and very low densities, and at higher temperatures of the order of 300–600 K and higher local densities, for example, surrounding particles in interstellar space. The excitation levels observed from the so-called unidentified infrared bands [30] have the most probable value close to $n = 80$. A comparison with the parameter values appropriate for the laboratory studies of cold RM shows that the density N_d is several orders of magnitude smaller in space than in laboratory experiments. On the other hand, for visible light, the wavenumber k_s is approximately 50 times larger than for the IR studies described here.

Equation (3) shows that a shift due to the stimulated Raman effect exists if the product $G_{ss}x$ is larger than unity. With Eq. (1) used for G_{ss} and with reasonable values also used for estimation of this factor above, it is possible to find a condition on the electric field strength of the light field. The distance covered by light in space is denoted by l. Then the inequality

$$\frac{k_s}{8m\epsilon\gamma c}\left(\frac{\partial\alpha}{\partial q}\right)_0^2 \geq \frac{\Delta\tilde{\nu}}{N_d l|E_L|^2} \qquad (4)$$

should be valid for the effect to exist. In this inequality, the space-related quantities are collected in the right hand side. The difference $\omega_L - \omega_s$ was replaced by $c\Delta\tilde{\nu}$, where $\Delta\tilde{\nu}$ is in wavenumbers. Assuming conservatively that γ is as large as the upper experimental limit found, $10^3\ s^{-1}$, we find that the left-hand side is equal to $2 \times 10^{-12}\ m^3\ V^{-2}$, with the other parameter values estimated as before. With the experimental values from the study of the cold RM described here, $\Delta\tilde{\nu} = 0.02\ cm^{-1}$, $N_d = 10^{17}\ m^{-3}$, $l = 0.25$ m, and $E_L = 90\ V\ m^{-1}$, the right-

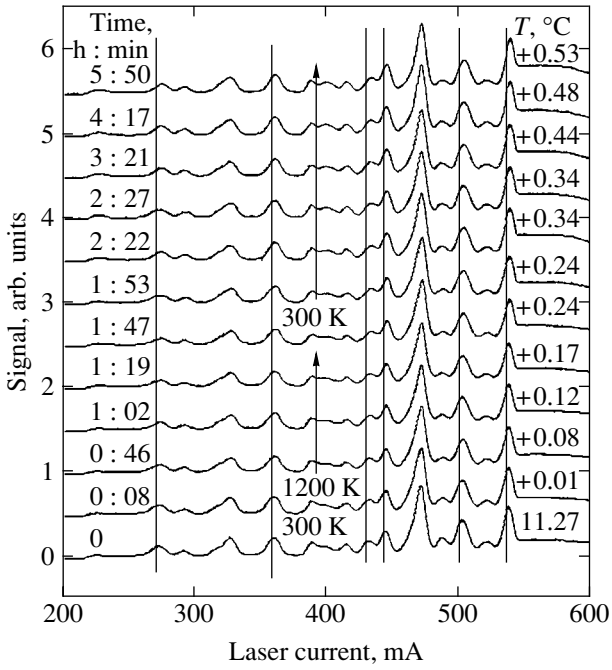

Fig. 3. Redshift of light from a diode laser at 1100 cm^{-1} passing through cold RM (in the top part of the figure). Time and the temperature of the water cooled interferometer base as well as the RM emitter temperature are given. The experiment was done at the air pressure 10^{-4} mbar in the RM chamber. The curves are consecutively shifted upwards to increase visibility.

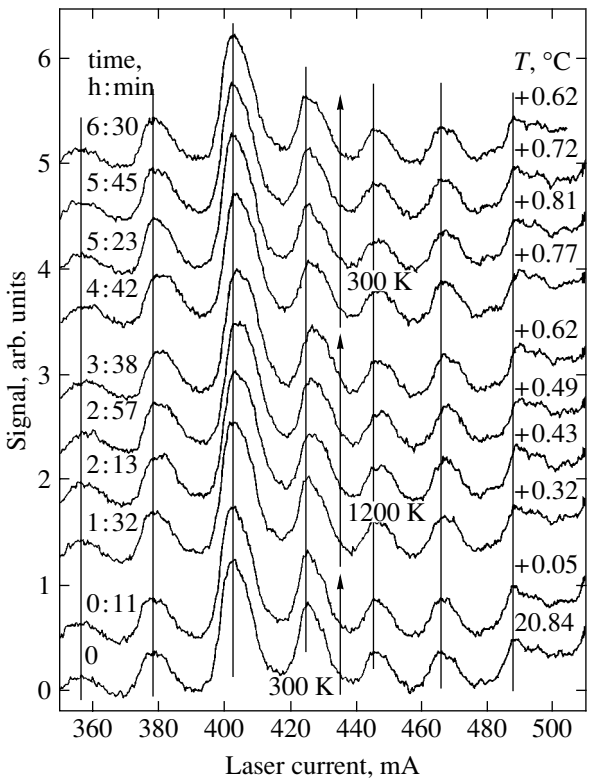

Fig. 4. Redshift of light from a diode laser at 1100 cm^{-1} reflected from a layer of RM on the inner face of the vacuum window. Time and the temperature of the FPI mirror holder and the RM emitter temperature are given. The experiment was conducted at an air pressure of 10^{-5} mbar in the RM chamber. The curves are consecutively shifted upwards to increase visibility. RM is slowly deexcited on the window when RM deposition is cancelled (at room temperature).

hand side becomes 1×10^{-20} m^3 V^{-2}. This is many orders of magnitude smaller than the left-hand side, as required by Eq. (4). Because some of the quantities are anyway somewhat uncertain, we may assume that the right-hand side of Eq. (4) in space should be as small as this value in experiments. (This is a very conservative estimate.) Then $\Delta\tilde{\nu} \approx 10^4$ cm^{-1} (the typical total summed shift in observations), $N_d = 10^6$ m^{-3} [42], and $l = 8 \times 10^8$ pc $= 2.5 \times 10^{25}$ m may be used, giving $E_L = 3 \times 10^{-3}$ V m^{-1}. The distance l used is smaller than the radius of the observable universe by about a factor of 10. This gives a light intensity of 2×10^{-8} W m^{-2} as the minimum intensity required to make the stimulated Raman process work, corresponding to the intensity of light from the Sun at our nearest star α Centauri. This is a very conservative estimate, based on the experimental results. If we instead use the condition that the right-hand side in Eq. (4) should only be smaller than the estimated value 2×10^{-12} m^3 V^{-2} of the left-hand side, the required light intensity may even be a factor of 10^9 smaller, thus larger than 2×10^{-17} W m^{-2} corresponding to the field strength $E_L = 10^{-7}$ V m^{-1}. This is the same as the intensity of the light from the Sun at the distance 4×10^4 pc, i.e., on the other side of our galaxy. Thus, a redshift due to stimulated Raman scattering develops even at very large distances from the source.

3.3. Redshifts

It is possible that the stimulated Raman process discussed here operates at the very low intensity levels in space, due to the extreme properties of intergalactic RM. It is of course interesting to investigate whether such an effect gives the behavior of ordinary redshifts, for example, whether the shift varies correctly with wavelength as

$$z = \frac{\lambda_{\text{obs}} - \lambda_{\text{em}}}{\lambda_{\text{em}}}, \tag{5}$$

which should be constant for a certain astronomical object independently of which spectral line is used for the determination. Thus, it is required that relation (5) is a constant, or that $\Delta\lambda/\lambda_L$ is a constant. This may be compared with the predictions from stimulated Raman theory. From Eq. (1), it follows that

$$\begin{aligned} G_{ss} &\propto \frac{k_s}{\omega_L - \omega_s} \propto \frac{\lambda_s^{-1}}{\lambda_L^{-1} - \lambda_s^{-1}} \\ &= \frac{\lambda_L}{\lambda_s - \lambda_L} = \frac{\lambda_L}{\Delta\lambda} \end{aligned} \tag{6}$$

holds, or that the observed behavior of the redshift is consistent with the stimulated Raman effect with a constant gain factor. The G_{ss} factor is not the real gain, as shown in [39] and cited above, but it is modified to the gain G that is nevertheless proportional to G_{ss}. This gain is constant independently of the shifting light intensities, e.g., for different spectral lines with different emitted intensities. Thus, the stimulated Raman effect gives the correct observed behavior.

From the description given here, it is also clear that the redshifting by the stimulated Raman process in RM is an additive process, given by the distance covered by light in the RM phase.

4. DISCUSSION

4.1. Quantum Effects

The main effect that may prevent the stimulated Raman effect from shifting the frequency of light continuously, as described above, is the quantal nature of excitations in the RM and the quantal nature of light. A finite lower bound to the size of the possible excitations in RM tends to prevent G_{ss} from reaching extremely large values, as can be seen from Eq. (1). The experimental redshifts or blueshifts are not observed to be

quantized at a level of 10^{-2} cm^{-1} or larger. This means that the quantum size is small. It is relevant to note that quantized redshifts are in fact observed, both for galaxies [1] and for quasars [2].

From the description in the theoretical section, a lower limit of the size of the quantized shifts could be 3×10^{-8} cm^{-1}. The quantized redshifts for nearby galaxies [1] instead suggest a quantum size of 6×10^{-6} cm^{-1} [3]. We use this value to make conservative estimates of the quantum effects. With the total summed shift 10^4 cm^{-1} in the visible range, the total number of shifts is then on the order of 10^9. If the distance traveled by the light is on the order of 10^{25} m, this means a shift of 6×10^{-6} cm^{-1} per 6×10^{15} m on average. Therefore, the shifts are very uncommon events. If the number of shifts is 10^9, the statistical variation in this number, the square root of this, is 3×10^4 on average. The statistical nature of the shifts is then not observed, but all light is shifted the same amount with an uncertainty on the order of 3×10^{-5}. This gives 0.3 cm^{-1} in a total shift of 10^4 cm^{-1}. Typical uncertainties in optical redshifts are ± 0.001 in z [43], giving ± 20 cm^{-1} for a typical optical line. Thus, the width of the observed lines are much larger than the widths resulting from the statistics of the redshift quanta.

4.2. Cosmological Arguments

In a recent book on cosmology [44], the four general cases of possible explanations of the redshifts of distant astronomical objects are summarized, with the fourth possibility "interaction (scattering, absorption)" being most relevant to the present discussion. It should be noted that stimulated Raman scattering was not considered explicitly, but only more "normal" scattering events were considered. The main arguments against the interaction processes given in [4] are as follows: (a) the resulting redshift should have an exponential dependence on distance, (b) the redshift $\Delta\lambda/\lambda$ would not be independent of frequency, and (c) a scattering process would smear out the light from distant sources, which is at variance with observations. The present model, based on the known physics of stimulated Raman processes, gives not an exponential but a linear dependence of the redshift on distance. As shown above, the redshift $\Delta\lambda/\lambda$ should be frequency-independent for the stimulated Raman process. The stimulated Raman process does not change the direction of light, and hence the final argument against a scattering mechanism of the stimulated Raman type is not valid either.

5. CONCLUSIONS

We conclude that the stimulated Raman mechanism for redshifting radiation in RM in space is a possible process to explain at least a part of the redshifts observed from distant astronomical objects. It gives the correct behavior, for example, concerning the frequency variation, the distance variation, and the direction of scattering. Further, the observed redshifts in cold RM in the laboratory are recalculated to astronomical distances and found to easily cover the range of the observed redshifts.

REFERENCES

1. B. N. G. Guthrie and W. M. Napier, Astron. Astrophys. **310**, 353 (1996).
2. G. Burbridge and W. M. Napier, Astron. J. **121**, 21 (2001).
3. L. Holmlid, Astrophys. Space Sci. **291**, 99 (2004).
4. T. E. Clarke, P. P. Kronberg, and H. Böhringer, Astrophys. J. **547**, L111 (2001).
5. S. Badiei and L. Holmlid, Mon. Not. R. Astron. Soc. **335**, L94 (2002).
6. S. Badiei and L. Holmlid, Mon. Not. R. Astron. Soc. **333**, 360 (2002).
7. J. Wang and L. Holmlid, Chem. Phys. Lett. **295**, 500 (1998).
8. S. Badiei and L. Holmlid, Int. J. Mass Spectrom. **220**, 127 (2002).
9. S. Badiei and L. Holmlid, Chem. Phys. **282**, 137 (2002).
10. J. Wang and L. Holmlid, Chem. Phys. **261**, 481 (2000).
11. J. Wang and L. Holmlid, Chem. Phys. **277**, 201 (2002).
12. S. Badiei and L. Holmlid, Phys. Lett. A **327**, 186 (2004).
13. S. Badiei and L. Holmlid, J. Phys.: Condens. Matter **16**, 7017 (2004).
14. É. A. Manykin, M. I. Ozhovan, and P. P. Poluéktov, Sov. Tech. Phys. Lett. **6**, 95 (1980).
15. É. A. Manykin, M. I. Ozhovan, and P. P. Poluéktov, Sov. Phys. Dokl. **26**, 974 (1981).
16. R. Svensson, L. Holmlid, and L. Lundgren, J. Appl. Phys. **70**, 1489 (1991).
17. R. Svensson and L. Holmlid, Surf. Sci. **269–270**, 695 (1992).
18. V. I. Yarygin, V. N. Sidelnikov, I. I. Kasikov, *et al.*, Pis'ma Zh. Éksp. Teor. Fiz. **77**, 330 (2003) [JETP Lett. **77**, 280 (2003)].
19. É. A. Manykin, M. I. Ozhovan, and P. P. Poluéktov, Zh. Éksp. Teor. Fiz. **102**, 804 (1992) [Sov. Phys. JETP **75**, 440 (1992)].
20. É. A. Manykin, M. I. Ozhovan, and P. P. Poluéktov, Zh. Éksp. Teor. Fiz. **102**, 1109 (1992) [Sov. Phys. JETP **75**, 602 (1992)].
21. J. Wang and L. Holmlid, Chem. Phys. Lett. **325**, 264 (2000).
22. L. Holmlid, Chem. Phys. **237**, 11 (1998).
23. L. Holmlid, Phys. Rev. A **63**, 013817 (2001).
24. L. Holmlid, Langmuir **17**, 268 (2001).
25. L. Holmlid, Astrophys. J. **548**, L249 (2001).
26. F. Olofson, S. Badiei, and L. Holmlid, Langmuir **19**, 5756 (2003).
27. L. Holmlid, Eur. Phys. J.: Appl. Phys. **26**, 103 (2004).

28. S. Badiei and L. Holmlid, Chem. Phys. Lett. **376**, 812 (2003).
29. L. Holmlid, J. Phys. B: At. Mol. Opt. Phys. **37**, 357 (2004).
30. L. Holmlid, Astron. Astrophys. **358**, 276 (2000).
31. L. Holmlid, Phys. Chem. Chem. Phys. **6**, 2048 (2004).
32. L. Holmlid, Appl. Phys. B **79**, 871 (2004).
33. J. C. White, in *Tunable Lasers*, Ed. by L. F. Mollenauer, J. C. White, and C. R. Pollock, 2nd ed. (Springer, Berlin, 1992), Topics in Applied Physics, Vol. 59.
34. R. Svensson and L. Holmlid, Phys. Rev. Lett. **83**, 1739 (1999).
35. A. Yariv, *Quantum Electronics*, 3rd ed. (Wiley, New York, 1989; Sovetskoe Radio, Moscow, 1973).
36. C. Åman, J. B. C. Pettersson, H. Lindroth, and L. Holmlid, J. Mater. Res. **7**, 100 (1992).
37. L. Holmlid and É. A. Manykin, Zh. Éksp. Teor. Fiz. **111**, 1601 (1997) [JETP **84**, 875 (1997)].
38. Y. R. Shen, *The Principles of Nonlinear Optics* (Wiley, New York, 1984; Nauka, Moscow, 1989).
39. Y. R. Shen and N. Bloembergen, Phys. Rev. A **137**, 1787 (1965).
40. L. Holmlid, J. Phys.: Condens. Matter **14**, 13469 (2002).
41. L. Holmlid, Chem. Phys. Lett. **367**, 556 (2003).
42. J. E. Dyson and D. A. Williams, *The Physics of the Interstellar Medium* (Inst. of Physics, Bristol, 1997).
43. R. C. Vermeulen, Y. M. Pihlström, W. Tschager, *et al.*, Astron. Astrophys. **404**, 861 (2003).
44. E. V. Linder, *First Principles of Cosmology* (Addison-Wesley, Harlow, 1997).